

Unifying Search and Recommendation in LLMs via Gradient Multi-Subspace Tuning

Jujia Zhao
j.zhao@liacs.leidenuniv.nl
Leiden University

Suzan Verberne
s.verberne@liacs.leidenuniv.nl
Leiden University

Zihan Wang
zhw.cypher@gmail.com
CISPA Helmholtz Center for
Information Security

Shuaiqun Pan
s.pan@liacs.leidenuniv.nl
Leiden University

Abstract

In this paper, we propose a generative framework for unifying search and recommendation (S&R) in large language models (LLMs). S&R are core to online platforms, addressing explicit intent through queries and modeling implicit intent from behaviors, respectively. Their complementary roles motivate a unified modeling paradigm. Early studies to unify S&R adopt shared encoders with task-specific heads, while recent efforts reframe item ranking in both S&R as conditional generation. The latter holds particular promise, enabling end-to-end optimization and leveraging the semantic understanding of LLMs. However, existing methods rely on full fine-tuning, which is computationally expensive and limits scalability. Parameter-efficient fine-tuning (PEFT) offers a more practical alternative but faces two critical challenges in unifying S&R: (1) gradient conflicts across tasks due to divergent optimization objectives, and (2) shifts in user intent understanding caused by overfitting to fine-tuning data, which distort general-domain knowledge and weaken LLM reasoning. To address the above issues, we propose Gradient Multi-Subspace Tuning (GEMS), a novel framework that unifies S&R with LLMs while alleviating gradient conflicts and preserving general-domain knowledge. GEMS introduces (1) **Multi-Subspace Decomposition**, which disentangles shared and task-specific optimization signals into complementary low-rank subspaces, thereby reducing destructive gradient interference, and (2) **Null-Space Projection**, which constrains parameter updates to a subspace orthogonal to the general-domain knowledge space, mitigating shifts in user intent understanding. Extensive experiments on benchmark datasets show that GEMS consistently outperforms the state-of-the-art baselines across both search and recommendation tasks, achieving superior effectiveness. Furthermore, GEMS is highly efficient and scalable, maintaining performance gains on LLMs with billions of parameters without introducing additional trainable weights.

ACM Reference Format:

Jujia Zhao, Zihan Wang, Shuaiqun Pan, Suzan Verberne, and Zhaochun Ren. 2025. Unifying Search and Recommendation in LLMs via Gradient Multi-Subspace Tuning. In . ACM, New York, NY, USA, 12 pages.



This work is licensed under a Creative Commons Attribution 4.0 International License.
Conference'17, Washington, DC, USA
© 2025 Copyright held by the owner/author(s).

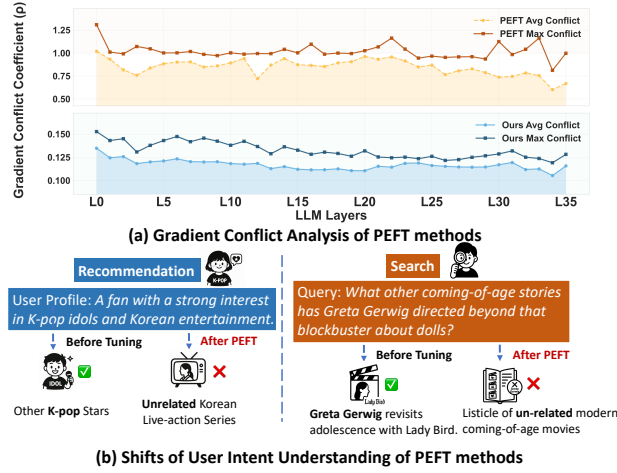


Figure 1: (a) Gradient conflict analysis across the layers of Qwen-3B under PEFT and our methods on the Qilin dataset. The Gradient Conflict Coefficient (ρ) [5] quantifies the degree of opposition between the gradients of the S&R tasks (see Section 5.3.2); lower values indicate less conflict. The results show that our method consistently achieves lower gradient conflicts compared to PEFT. (b) Shifts in user intent understanding in real-world S&R.

1 Introduction

Recommender systems and search engines are two integral parts of modern online service platforms, both fundamentally aiming to model and satisfy user information needs [30, 37, 40]. Their shared objective reveals a natural connection, while their complementary user behaviors offer opportunities for mutual enhancement [22]. Search queries capture users' short-term intents that can inform timely recommendations, whereas recommendation models encode long-term preferences that can improve the personalization of search results [32]. Integrating the two within a unified framework therefore represents a promising direction, enabling richer user modeling and potentially improving the overall effectiveness of both tasks [35].

Early attempts to unify S&R adopt shared transformer modules to process input features (e.g., user interaction histories or queries) and use task-specific heads to predict relevance scores between users and candidate items, followed by a ranking step to identify

the target item [22, 35]. Although these methods show promise, they require considerable manual effort in designing model architectures and task-specific heads, which limits their scalability and practicality. In addition, the absence of end-to-end optimization makes them prone to local optima [14]. Recent advances instead employ generative models that reframe ranking as conditional generation, using pre-trained language models (PLMs) to directly generate target item identifiers conditioned on user queries or interaction histories [16]. These approaches are readily adaptable to different PLM backbones and support end-to-end training, offering higher flexibility and a more favorable optimization landscape than earlier paradigms. Furthermore, generative methods naturally inherit the strong semantic understanding and reasoning capabilities of PLMs, enabling richer modeling of both user intent and item representations [23].

However, existing generative methods rely on full fine-tuning, which limits generalization and scalability and leads to substantial computational and memory costs when applied to prevailing large language models (LLMs). To address these limitations, recent studies explore parameter-efficient fine-tuning (PEFT) techniques that update only a small subset of parameters (e.g., low-rank adapters or prefix tokens) while keeping most backbone weights frozen, thereby reducing the resource demands of large-scale adaptation [10]. Despite these advantages, PEFT presents two critical challenges when applied to unified S&R tasks: (1) **Gradient conflicts across tasks**. As shown in Figure 1(a), significant disagreement between task gradients is observed across multiple LLM layers. This arises because search and recommendation pursue inherently different objectives: search focuses on modeling query-item relevance within the current query context, whereas recommendation emphasizes capturing long-term user preferences from historical interactions. These conflicting optimization signals lead to contradictory gradient directions, resulting in unstable training and degraded performance for both tasks. (2) **Shifts in user intent understanding**. During PEFT-based adaptation, overfitting to limited fine-tuning data often induces a semantic distribution shift in the representation space [6]. This shift disrupts general-domain knowledge and weakens the model's intrinsic language understanding and reasoning abilities to interpret user intent. Consequently, the model may generate incorrect or inconsistent outputs even for queries it previously handled correctly (see Figure 1(b)).

To address abovementioned challenges, we introduce a **Gradient Multi-Subspace Tuning** (GEMS) framework that unifies S&R within LLMs while mitigating gradient conflict and preserving general-domain knowledge. GEMS is built on the core idea of **subspace tuning**: rather than updating all parameters along raw gradient directions, it projects gradients into a set of dominant low-rank subspaces learned from gradient statistics for optimization [41]. The resulting updates are then projected back into the full parameter space, substantially reducing the overall tuning cost. Compared with PEFT methods, subspace tuning eliminates the restrictive low-rank assumptions imposed by reparameterization [31] and significantly reduces memory overhead, as only the optimizer states and gradients within the low-rank subspace need to be maintained.

Building on subspace tuning, GEMS introduces two key components to tackle the above challenges: (1) **Multi-subspace decomposition** further organizes the updates into three complementary subspaces: a shared subspace capturing information consistently

useful to both tasks, and two task-specific subspaces that encode signals unique to S&R, respectively. By explicitly disentangling shared and task-specific signals, GEMS mitigates gradient conflicts: updates along directions agreed upon by both tasks are routed to the shared subspace, while potentially conflicting signals are confined to their respective task-specific subspaces. Since these task-specific subspaces are constructed from inherently different gradient patterns, they exhibit minimal geometric overlap, substantially reducing the chance of destructive gradient interference when their updates are combined. An adaptive gating mechanism further balances their contributions over training based on task dynamics, improving optimization stability. (2) **Null-space projection** constrains updates to be orthogonal to the general-domain knowledge space, thereby preserving the model's inherent language understanding and reasoning capabilities. Specifically, GEMS estimates the principal representation space of the backbone model using general-domain pre-trained data and projects the combined gradient onto the null space of this knowledge space, effectively limiting representational drift and maintaining robust user intent understanding. To evaluate the effectiveness and efficiency of GEMS, we conduct extensive experiments on benchmark datasets spanning both search and recommendation scenarios. The results show that GEMS consistently outperforms strong baselines, including state-of-the-art S&R models and leading PEFT approaches.

Our main contributions are summarized as follows: (1) To the best of our knowledge, ours is the first study to adapt LLMs with billions of parameters for unified S&R without full fine-tuning, enabling efficient parameter updates and knowledge preservation. (2) We introduce multi-subspace decomposition, which disentangles shared and task-specific optimization signals to mitigate gradient conflicts by separating consistent and conflicting gradient directions into complementary low-rank subspaces. (3) We develop null-space projection, which constrains parameter updates to be orthogonal to the general-domain knowledge space, reducing representational drift and preserving the model's language understanding and reasoning capabilities. (4) We conduct extensive experiments across multiple benchmark datasets and LLM backbones, demonstrating that GEMS outperforms competitive baselines in S&R performance, training efficiency, mitigation of gradient conflicts, and preservation of general-domain knowledge.

2 Related Work

Unifying search and recommendation. Unifying search and recommendation (S&R) within a single model promises richer user modeling and mutual gains, and has therefore attracted growing attention [16, 38, 39, 42]. Early attempts share transformer modules while attaching task-specific heads that score user-item relevance, followed by a final ranking step [35, 36]. For example, UnifiedSSR [32] jointly models user behavior history in S&R scenarios using a parameter-sharing dual-branch network and an intent-oriented session module. UniSAR [22] models fine-grained user behavior transitions between S&R through extraction, alignment, and fusion. While effective, these methods demand substantial manual design and lack end-to-end optimization, making them vulnerable to local optima [14]. More recent efforts employ generative models, leveraging PLMs to directly generate target item identifiers

conditioned on user queries or interaction histories [15]. Specifically, BSR [16] jointly trains generative models for S&R tasks using atomic item identifiers. GenSAR [23] unifies generative S&R by designing dual-purpose semantic and collaborative item identifiers. While current generative methods implements greater practicality and end-to-end optimization, they rely on full fine-tuning, which faces computational and memory costs when applying to LLMs.

Multi-task learning in LLMs. Although not yet widely applied to unifying S&R, LLMs have emerged as powerful backbones for multi-task learning due to their strong contextual reasoning and generalization abilities [2, 18, 29]. By leveraging instruction-based formulations and shared semantic representations, LLMs can jointly learn multiple related tasks, enhancing overall performance [27]. Existing approaches can be grouped into two main directions. (1) Unified instruction-based fine-tuning, which fully shares model parameters across tasks and formats each task as a natural language instruction [11, 21, 28]. For instance, T0 [20] reformulates diverse datasets into prompted forms and fine-tunes a single model, achieving strong generalization to unseen tasks. While effective, this paradigm demands careful balancing of heterogeneous data and suffers from task interference when objectives conflict [3]. (2) Parameter-efficient multi-task learning, which introduces light-weight modules or experts for each task while sharing a common backbone [8, 17, 34]. For instance, LoRA-MoE [4] enhances multi-task learning by integrating a plugin Mixture-of-Experts architecture with specialized LoRA experts, utilizing localized balancing constraints to dynamically route and dedicate expert groups for distinct downstream tasks and knowledge retention. While these modular approaches mitigate gradient conflicts, they introduce additional complexity and cost (e.g. routing mechanisms and multiple modules), and their performance hinges on effective assignment of tasks to the right experts [7, 13]. In contrast, our proposed GEMS framework is based on subspace tuning, requiring no additional routing or auxiliary modules. Additionally, GEMS learns task-specific subspaces derived from task statistics, effectively capturing unique optimization directions for each task.

In this work, we efficiently unify S&R within LLMs. The most closely related studies include [15, 16, 23]. However, they face two major challenges: (i) gradient conflict across tasks; and (ii) shifts in user-intent understanding. Our proposed GEMS, which incorporates multi-subspace decomposition and null-space projection to alleviate gradient conflicts and preserve accurate user-intent understanding.

3 Preliminaries

Unifying S&R. We formulate the task of unifying S&R as learning a single model that integrates users' historical S&R interactions to perform either task according to user needs. In the search setting, the objective is to retrieve documents relevant to a user's query while leveraging their historical S&R interactions. In the recommendation setting, the objective is to suggest items based on the same historical interactions. Formally, let \mathcal{U} and \mathcal{I} denote the sets of users and item identifiers. For each user $u \in \mathcal{U}$, the model aims to generate the target item identifier(s) given: (1) an interaction history $H_u = (i_1, b_1), (i_2, b_2), \dots, (i_N, b_N)$, where $i_n \in \mathcal{I}$ and $b_n \in \{\text{src, rec}\}$ denote the n -th item in the interaction history and

its interaction type (i.e., search or recommendation), respectively; and (2) a query q , which is provided in the search setting but left empty in recommendation.

Generative model for unifying S&R. To unify search and recommendation (S&R) within a generative framework, we formulate both tasks as conditional text generation. All input information is converted into a unified structured prompt x , which is tokenized and fed into the model for instruction tuning. The model then generates the target item identifier to reflect user preferences through constrained generation. The training objective minimizes the negative log-likelihood of the user's preference (i.e., the target item i) conditioned on the input instruction x in an autoregressive manner:

$$\min_{\Theta} \mathcal{L}(\Theta) = - \sum_{t=1}^{|i|} \log P_{\Theta}(i_t | i_{<t}, x), \quad (1)$$

where Θ denotes the model parameters, i_t is the t -th token of the target item i , and $i_{<t}$ represents all tokens preceding i_t . During optimization, we compute gradients and update the model parameters using the Adam optimizer [12]. During inference, the model employs beam search to generate the top- K ranked items, which serve as the final S&R results.

4 Method

In this section, we first introduce the core concept of our proposed Gradient Multi-Subspace Tuning (GEMS) framework and its underlying principle of subspace tuning, which enables efficient full-parameter optimization for LLMs (see Section 4.1). We then present the two main components of GEMS, as illustrated in Figure 2: multi-subspace decomposition (see Section 4.2) and null-space projection (see Section 4.3). Finally, we describe the overall training algorithm and analyze the memory and optimization efficiency of GEMS in comparison with the widely used PEFT approach, *i.e.*, LoRA [10] (see Section 4.4).

4.1 Subspace tuning

GEMS is built upon the concept of subspace tuning [41], which enables gradient updates within low-rank subspaces, thereby ensuring efficient training in the LLM setting. At each training step t , for every trainable layer of the LLM with weight matrix $W_t \in \mathbb{R}^{m \times n}$, we compute the backpropagated gradient matrix $G_t = -\nabla_{W_t} \mathcal{L}(\Theta_t) \in \mathbb{R}^{m \times n}$. Instead of directly updating W_t using G_t following the Adam optimizer [12], as in conventional approaches, we project G_t onto a low-rank subspace spanned by a small set of principal directions of the gradient statistics. Specifically, we perform singular value decomposition (SVD) on G_t :

$$G_t = U \Sigma V^T, \quad (2)$$

and retain the top- r singular vectors $U_r \in \mathbb{R}^{m \times r}$ as the basis of the subspace, where r denotes the subspace rank. The projected gradient is then obtained as:

$$G_t^{(r)} = U_r^T G_t. \quad (3)$$

Next, optimization is performed entirely within this r -dimensional subspace. Following the procedure of the Adam optimizer [12], we maintain first- and second-order moment estimates $M^{(r)}$ and $V_t^{(r)}$

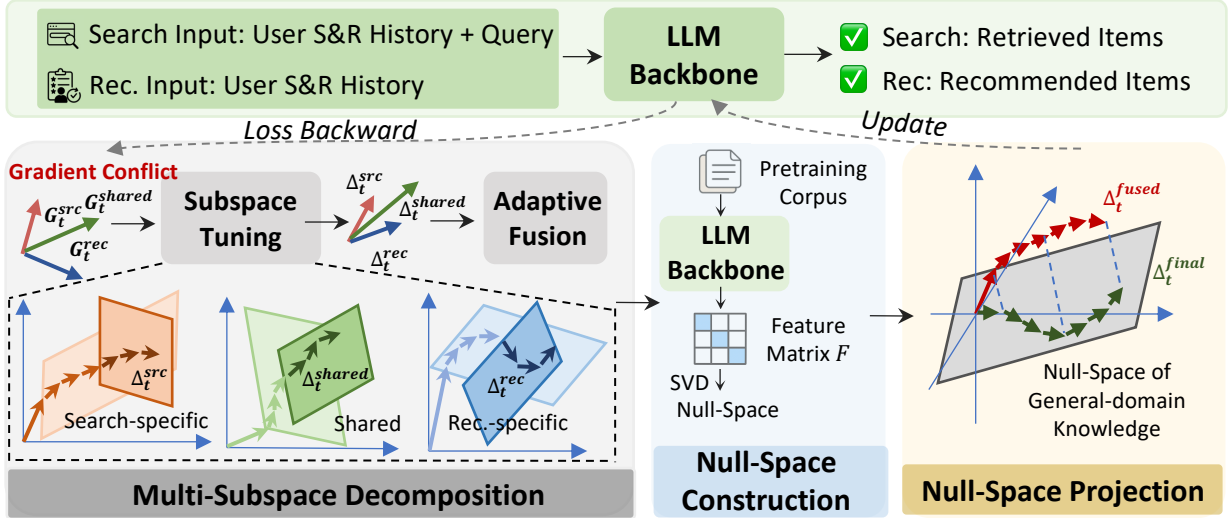


Figure 2: An overview of GEMS. During unified S&R training, task gradients are routed through multi-subspace decomposition and adaptively fused, then projected onto the null-space of pre-trained knowledge to preserve general-domain understanding.

in this low-rank subspace:

$$M_t^{(r)} = \beta_1 M_{t-1}^{(r)} + (1 - \beta_1) G_t^{(r)}, \quad (4)$$

$$V_t^{(r)} = \beta_2 V_{t-1}^{(r)} + (1 - \beta_2) (G_t^{(r)} \odot G_t^{(r)}), \quad (5)$$

with bias correction:

$$\hat{M}_t^{(r)} = \frac{M_t^{(r)}}{1 - \beta_1^t}, \quad \hat{V}_t^{(r)} = \frac{V_t^{(r)}}{1 - \beta_2^t}, \quad (6)$$

where $\beta_1, \beta_2 \in [0, 1]$ are decay rates in Adam Optimizer. The update in the subspace is given by:

$$\Delta_t^{(r)} = -\eta \cdot \frac{\hat{M}_t^{(r)}}{\sqrt{\hat{V}_t^{(r)}} + \epsilon}. \quad (7)$$

Finally, we map this update back into the full parameter space through the basis U_r :

$$\Delta_t = \alpha \cdot U_r \Delta_t^{(r)}, \quad (8)$$

and apply it to all parameters:

$$W_{t+1} = W_t + \Delta_t. \quad (9)$$

where the scaling factor α controls the magnitude of the low-rank update. In this way, optimization proceeds along a few principal directions while still influencing the entire parameter space. To further reduce computational cost practically, the SVD is refreshed only once every T_{svd} steps.

This subspace-based procedure significantly reduces the number of gradient directions, thereby lowering both computational and memory costs. Moreover, by filtering gradients through principal directions, subspace tuning suppresses noisy components and enhances training stability, while retaining much of the expressive capacity of full fine-tuning.

4.2 Multi-subspace decomposition

To address gradient conflicts that arise when jointly optimizing search and recommendation objectives, we design a *multi-subspace*

decomposition strategy. The key idea is to decompose the optimization space into multiple low-rank subspaces that separate shared and task-specific gradient signals. Directions agreed upon by both tasks are preserved in a shared subspace to promote common representation learning, while task-divergent directions are confined to their respective task-specific subspaces. This separation prevents incompatible updates from competing within the same representational space and thus mitigates destructive interference. Moreover, since each task-specific subspace is derived from distinct gradient statistics, their geometric overlap remains minimal, allowing stable and independent optimization dynamics across tasks. As a result, the model learns generalizable shared representations without compromising task-specific adaptation.

Formally, let \mathcal{L}_{src} and \mathcal{L}_{rec} denote the search and recommendation losses, respectively. At each training step t , we compute the corresponding gradients matrix:

$$G_t^{src} = -\nabla_{W_t} \mathcal{L}_{src}(\Theta), \quad G_t^{rec} = -\nabla_{W_t} \mathcal{L}_{rec}(\Theta). \quad (10)$$

We further define the shared gradient as:

$$G_t^{shared} = -\nabla_{W_t} (\mathcal{L}_{src}(\Theta) + \mathcal{L}_{rec}(\Theta)). \quad (11)$$

Shared and task-specific subspaces. Based on these gradients, GEMS constructs one shared subspace and two task-specific subspaces to disentangle common and distinct optimization directions. The **shared subspace** captures gradient directions beneficial to both tasks, including general user preference patterns (e.g., broad interest categories) and semantic information from interacted items (e.g., textual representations). The **search-specific subspace** focuses on signals unique to search, such as modeling semantic intent in queries and aligning user queries with item content. The **recommendation-specific subspace** emphasizes signals unique to recommendation, such as user long-term preferences and collaborative filtering patterns from historical interactions. Following the subspace tuning procedure in Section 4.1, the corresponding

updates Δ_t^{shared} , Δ_t^{src} , and Δ_t^{rec} are derived from their respective gradients G_t^{shared} , G_t^{src} , and G_t^{rec} according to Eq. 2–8.

Adaptive fusion of subspaces. After obtaining the gradient updates from each subspace, the three projected gradients are then fused through an adaptive gating mechanism. In this design, the shared subspace always contributes to the final update with a fixed weight of 1, ensuring that task-invariant signals are consistently preserved. By contrast, the search- and recommendation-specific subspaces are combined with dynamic weights $\alpha_{\text{src}}, \alpha_{\text{rec}} \geq 0$ that satisfy

$$\alpha_{\text{src}} + \alpha_{\text{rec}} = 1. \quad (12)$$

The fused update applied to the parameter set is therefore

$$\Delta_t^{\text{fused}} = \Delta_t^{\text{shared}} + \alpha_{\text{src}} \Delta_t^{\text{src}} + \alpha_{\text{rec}} \Delta_t^{\text{rec}}. \quad (13)$$

and apply it to all parameters:

$$W_{t+1} = W_t + \Delta_t^{\text{fused}}. \quad (14)$$

To determine the gating weights, we design a lightweight neural network conditioned on task-level statistics that reflect the relative learning states of the two tasks. In particular, we extract three types of normalized ratios: (i) the relative magnitudes of task losses, (ii) the relative gradient norms of the two tasks, and (iii) the relative sample sizes within the current batch. These ratios collectively form a feature vector

$$z = [s^{\text{loss}}, s^{\text{grad}}, s^{\text{sample}}]. \quad (15)$$

The adaptive gating network $f_{\phi}(\cdot)$ is implemented as a two-layer perceptron with ReLU activations:

$$h = \sigma(W_1 z + b_1), \quad o = W_2 h + b_2, \quad (16)$$

where $\sigma(\cdot)$ is the ReLU function, and $\phi = \{W_1, b_1, W_2, b_2\}$ are learnable parameters. This design enables the gating module to non-linearly model the relationships among multiple task indicators and to infer which subspace should receive greater emphasis at each step. In essence, the gating network serves as a meta-controller that monitors the training dynamics of both tasks and adaptively allocates learning capacity: when one task exhibits higher loss or unstable gradients, its corresponding subspace receives a smaller weight, thereby stabilizing joint optimization and preventing one task from dominating the shared representation learning.

Finally, the gating weights are obtained by a temperature-scaled softmax:

$$\alpha = \text{softmax}\left(\frac{o}{\tau}\right), \quad (17)$$

where τ is a gate temperature factor and controls the sharpness of the gating distribution. Thus, $\alpha = [\alpha_{\text{src}}, \alpha_{\text{rec}}]$ defines the adaptive combination coefficients for the three subspace gradients in Eq. (13). This enables the framework to adaptively balance shared and task-specific updates during training, ensuring stable convergence and effective coordination between S&R learning.

4.3 Null-space projection

As stated in the Section 1, PEFT methods may cause a shift in the user intent understanding, distribution of pre-trained knowledge, leading to general-domain knowledge disruption and erosion of the semantic and reasoning abilities of the backbone LLM. To mitigate this problem, we introduce a *null-space projection* that preserves

general-domain knowledge while still enabling effective adaptation to unified S&R tasks.

The key idea is to identify the principal representation space of the backbone LLM, which corresponds to its general-domain knowledge, and to prevent fine-tuning updates from moving along these dominant directions. To achieve this, updates are projected into the complementary subspace (the null space), which poses a lower risk of disturbing pre-trained semantics [6].

To estimate the principal directions of the backbone LLM’s pre-trained representation space (i.e., those most responsible for encoding general-domain knowledge), we construct a feature matrix $F \in \mathbb{R}^{n \times C}$ by collecting hidden states from the backbone LLM on a representative general-domain corpus C . Here, n denotes the dimensionality of the layer’s hidden representation (the input dimension of the corresponding weight matrix $W_t \in \mathbb{R}^{m \times n}$), and C is the number of input instances from C . We then apply singular value decomposition (SVD) to the covariance matrix FF^T :

$$U_{\text{pre}} \Sigma V_{\text{pre}}^T = \text{SVD}(F(F^T)). \quad (18)$$

The purpose of this step is to identify a set of orthogonal basis vectors ordered by their contribution to the variance of pre-trained principal representations. Intuitively, the top- k singular vectors in U_{pre} capture the dominant semantic directions most critical to general reasoning and semantic understanding.

Following this, we define the projection matrix onto the null-space of U_{pre}^k (the top- k singular vectors of U_{pre}) as:

$$P_{\perp} = U_{\text{pre}}^k U_{\text{pre}}^{k\top}, \quad (19)$$

which removes any component of an update that aligns with the dominant pre-trained directions. Since the projection matrix P_{\perp} depends solely on the general-domain knowledge, it only needs to be computed once during the preparation stage before training, thereby reducing computational cost. Given a fused gradient update Δ_t^{fused} at training step t , the final update is obtained by:

$$\Delta_t^{\text{final}} = P_{\perp} \Delta_t^{\text{fused}}. \quad (20)$$

This procedure ensures that gradient updates avoid interfering with the principal directions associated with pre-trained representations, thereby reducing knowledge shift and preserving the semantic structures acquired during pre-training. As a result, the model adapts to S&R tasks mainly along directions less aligned with prior knowledge, striking a balance between efficient fine-tuning and knowledge preservation.

4.4 Training algorithm

We list the detailed training algorithm in Algorithm 1 (Appendix). At each step t , a mini-batch is sampled to compute task-specific losses \mathcal{L}_{src} and \mathcal{L}_{rec} , yielding gradient matrices G_t^{src} and G_t^{rec} , as well as a shared gradient G_t^{shared} . These gradients define three low-rank subspaces (i.e., shared, search-specific, and recommendation-specific), whose bases are obtained via SVD and refreshed every T_{svd} steps. Parameter updates $(\Delta_t^{\text{shared}}, \Delta_t^{\text{src}}, \Delta_t^{\text{rec}})$ are computed by projecting gradients into these subspaces and are optimized using independent Adam optimizers. An adaptive gating mechanism then fuses their contributions into Δ_t^{fused} , which undergoes a null-space

projection to obtain Δ_t^{final} , ensuring orthogonality to the general-domain knowledge space. The final update Δ_t^{final} is applied to the model parameters W_t , and the process repeats until convergence. **Efficiency.** Unlike PEFT methods, which introduce additional low-rank matrices per adapted layer, GEMS requires no extra trainable weights beyond the backbone. All learning occurs through projected gradients within compact subspaces, leaving the inference-time parameter count identical to the base model. This design considerably reduces memory usage and deployment overhead. During training, only optimizer states for three low-rank subspaces (one shared and two task-specific) are maintained, keeping the total footprint low. Although multiple subspaces slightly increase optimizer states compared to PEFT, the absence of additional parameters results in a lighter and more efficient model overall. A detailed comparison of computational and memory complexity with LoRA is provided in Table 5 in the Appendix.

5 Experiments

We address the following research questions: (RQ1) Does GEMS outperform state-of-the-art baselines on the S&R tasks? (RQ2) Do the components of GEMS contribute to its effectiveness? (RQ3) Can GEMS mitigate gradient conflicts and shifts in user intent understanding for S&R? (RQ4) How do hyperparameters influence the performance of GEMS?

5.1 Experimental setup

Datasets. We evaluate GEMS on two publicly available datasets containing both S&R histories: (1) **Amazon**¹ is a large product review dataset with user reviews and metadata (e.g., titles and descriptions). We use the *Electronics* 5-core subset, which provides reviews and ratings for electronic devices. Following prior work [22, 24], we synthesize search behaviors by extracting queries from item category hierarchies and pairing them with purchase records to form user–query–item triples, then apply a leave-one-out splitting strategy. This procedure has been widely used to evaluate unified S&R models in the absence of real-world datasets [1]. (2) **Qilin**² is a dataset collected from a social media application, a popular content-sharing platform that integrates both S&R behaviors, including real queries and item descriptions. Following [22], we retain only users with both behaviors. The dataset statistics is shown in Table 4 (Appendix).

Baselines. We compare GEMS with state-of-the-art methods in recommendation, search, and unifying S&R. We also select mainstream PEFT methods. **Recommendation baselines:** (1) **NCF** [9] replaces the inner product in matrix factorization with a neural architecture to model complex user–item interactions. (2) **TIGER** [19] assigns discrete Semantic IDs to items and trains a seq2seq model to predict the next item’s ID in a user’s history. (3) **LETTER** [26] integrates hierarchical semantics, collaborative signals, and code assignment diversity into item identifiers for LLM-based generative recommendation. **Search baselines:** (4) **ANCE** [33] improves dense retrieval by mining hard negatives via an asynchronously updated ANN index. (5) **WebUltron** [43] introduces an end-to-end generative retrieval framework with semantically rich item

identifiers. (6) **GenRet** [25] tokenizes items into learnable semantic identifiers. **Unifying baselines:** (7) **UnifiedSSR** [32] shares information across scenarios/views and models user intent with self-supervised session discovery. (8) **BSR** [16] uses atomic item IDs to jointly train generative models for search and recommendation. (9) **Sem-BSR** [15] learns effective Semantic IDs by jointly fine-tuning a bi-encoder on both tasks. (10) **GenSAR** [23] designs dual-purpose semantic and collaborative item identifiers to unify generative search and recommendation.

PEFT methods: (11) **LoRA** [10] reparameterizes weight matrices into low-rank components and trains lightweight adapters, enabling efficient adaptation without modifying the entire parameter space. (12) **LoRA-MoE** [4] introduces a plugin Mixture-of-Experts (MoE) architecture with LoRA experts and localized balancing constraints to prevent LLMs’ world knowledge forgetting during fine-tuning.

Implementation details. Following prior work [22, 32, 35], we randomly sample 99 negative items per user and combine them with the ground-truth item to form candidate lists. All models rank these candidates, and we evaluate top- K S&R performance using Hit@ K and NDCG@ K with $K = \{5, 10\}$. Hyperparameters for baselines are tuned within the ranges reported in their original papers. For fairness, we apply constrained beam search to all generative baselines, ensuring outputs are restricted to valid candidates. We compare our method with generative unifying S&R baselines across two LLM backbones: Flan-T5-base³ and Qwen2.5-3B-Instruct⁴. For the Flan-T5-base model, we perform full fine-tuning on all generative methods. For the Qwen2.5-3B-Instruct model, we implement PEFT across all generative methods. We use the Wikipedia⁵ dataset as the general-domain corpus C when conducting null-space projection. The best hyperparameters are selected through grid search over the following ranges: the scale factor α is tuned in $\{0.5, 1, 2, 3, 4\}$, the gate temperature factor τ in $\{0.1, 0.5, 1, 2, 3\}$, and the subspace rank⁶ in $\{256, 512, 1024\}$.

5.2 Results on S&R (RQ1)

We conduct a comprehensive comparison of GEMS against a range of baselines across both S&R tasks under different LLM backbones. As summarized in Table 1 and Table 2, our experiments yield three key observations: (1) Unifying S&R remains challenging. Unified baselines often underperform specialized models, underscoring severe gradient conflicts between the two objectives, where updates that benefit one task may degrade the other when a shared representation is enforced. This effect is particularly pronounced with T5-base, where full fine-tuning exposes all parameters (embeddings, attention, and feed-forward layers) to both tasks, amplifying cross-task interference. (2) GEMS achieves the highest performance across nearly all datasets and tasks. The gains are particularly notable under T5-base, where it outperforms the best specialized baselines by margins ranging from 68% to over 470% on Hit@5. This superior

³<https://huggingface.co/google/flan-t5-base>.

⁴<https://huggingface.co/Qwen/Qwen2.5-3B-Instruct>.

⁵<https://huggingface.co/datasets/wikimedia/wikipedia/viewer/20231101.en>.

⁶Each task-specific subspace rank is set to half of the shared subspace rank. This design encourages compact specialization by allowing task-specific parameters to capture residual variations around the shared representation while preventing over-parameterization.

¹<https://jmcauley.ucsd.edu/data/amazon>.

²<https://github.com/RED-Search/Qilin>.

Table 1: Results on S&R. Backbone model is T5-base. The best and second-best results are highlighted in bold and underlined fonts, respectively. * indicates that the best result is statistically significantly better than the second-best (t-test, $p < 0.01$).

Task	Method	Qilin				Amazon			
		Hit@5	Hit@10	NDCG@5	NDCG@10	Hit@5	Hit@10	NDCG@5	NDCG@10
Recommendation	NCF	0.1497	0.2019	0.1267	0.1433	0.1718	0.2035	0.1009	0.1273
	TIGER	<u>0.2548</u>	<u>0.3052</u>	<u>0.1971</u>	<u>0.2091</u>	<u>0.2019</u>	0.2581	<u>0.1494</u>	<u>0.1675</u>
	LETTER	0.2116	0.2577	0.1605	0.1723	0.2014	0.2582	0.1491	0.1674
	UnifiedSSR	0.1531	0.2171	0.1325	0.1446	0.1477	0.1986	0.0923	0.1313
	BSR	0.2089	0.2432	0.1587	0.1673	0.2004	0.2568	0.1474	0.1656
	Sem-BSR	0.2437	0.2936	0.1904	0.2033	<u>0.2019</u>	<u>0.2584</u>	0.1484	0.1664
	GenSAR	0.2168	0.2527	0.1678	0.1771	0.2008	0.2575	0.1478	0.1661
	Ours	0.4285*	0.5121*	0.3251*	0.3465*	0.4025*	0.5159*	0.2975*	0.3341*
Search	ANCE	0.0209	0.0324	0.0114	0.0153	0.0487	0.0979	0.0285	0.0441
	WebUltron	0.0228	<u>0.0390</u>	0.0136	0.0185	0.2213	0.2554	0.1962	0.2071
	GenRet	<u>0.0262</u>	0.0378	<u>0.0156</u>	0.0194	<u>0.4198</u>	0.4205	<u>0.3995</u>	<u>0.3998</u>
	UnifiedSSR	0.0138	0.0251	0.0097	0.0227	0.1866	0.2481	0.1305	0.1558
	BSR	0.0153	0.0290	0.0137	0.0259	0.2058	<u>0.3215</u>	0.1702	0.2075
	Sem-BSR	0.0261	0.0606	0.0152	<u>0.0263</u>	0.2023	0.2603	0.1496	0.1683
	GenSAR	0.0141	0.0286	0.0090	0.0136	0.4032	<u>0.4608</u>	0.3170	0.3686
	Ours	0.1511*	0.1922*	0.0989*	0.1122*	0.8399*	0.8456*	0.8000*	0.8018*

Table 2: Results on S&R. Backbone model is Qwen-3B. The best and second-best results are highlighted in bold and underlined fonts, respectively. * indicates that the best result is statistically significantly better than the second-best (t-test, $p < 0.01$).

Task	Method	Qilin				Amazon			
		Hit@5	Hit@10	NDCG@5	NDCG@10	Hit@5	Hit@10	NDCG@5	NDCG@10
Recommendation	TIGER	0.2469	0.3008	0.1858	0.2001	<u>0.1886</u>	0.2487	0.1375	0.1571
	LETTER	0.1845	0.2446	0.1338	0.1532	0.1845	0.2446	0.1338	0.1532
	BSR	0.1087	0.1356	0.0813	0.0881	0.0837	0.1215	0.0598	0.0703
	Sem-BSR	0.2432	0.2891	0.1893	0.2009	0.1300	0.1938	0.0873	0.1078
	GenSAR	0.1168	0.1625	0.0832	0.0971	0.0916	0.1382	0.0625	0.0775
	Sem-BSR-MoE	<u>0.3061</u>	<u>0.3419</u>	0.2491	0.2562	0.1812	0.2799	0.1846	<u>0.1823</u>
	Ours	0.3499*	0.4219*	0.2648*	0.2837*	0.3686*	0.4743*	0.2717*	0.3056*
	WebUltron	0.0369	0.0535	0.0218	0.0271	0.1754	0.2423	0.1243	0.1459
Search	GenRet	<u>0.0510</u>	<u>0.0776</u>	<u>0.0306</u>	<u>0.0393</u>	0.1598	0.2309	0.1107	0.1336
	BSR	0.0124	0.0211	0.0075	0.0102	0.1732	0.2391	0.1237	0.1445
	Sem-BSR	0.0279	0.0469	0.0196	0.0255	0.3132	0.3515	<u>0.2719</u>	0.2843
	GenSAR	0.0155	0.0224	0.0101	0.0123	0.1997	0.2259	0.1785	0.1868
	Sem-BSR-MoE	0.0328	0.0532	0.0258	0.0313	<u>0.3291</u>	<u>0.3729</u>	0.2902	<u>0.2893</u>
	Ours	0.0552*	0.0780*	0.0374*	0.0447*	0.3510*	0.4570*	0.2596	0.2938*

performance can be attributed to GEMS's multi-subspace decomposition and null-space projection. (3) Compared to mainstream PEFT baselines and PEFT-MoE variants, GEMS mostly achieves the best results. These results demonstrate that GEMS can provide greater performance gains while maintaining efficiency. Notably, its ability to outperform MoE-enhanced PEFT suggests that merely increasing routing capacity is insufficient to resolve cross-task interference.

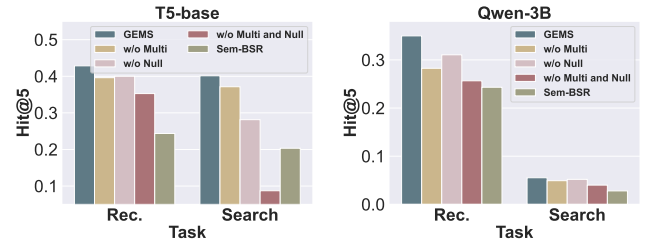


Figure 3: Ablation study of GEMS on Qilin.

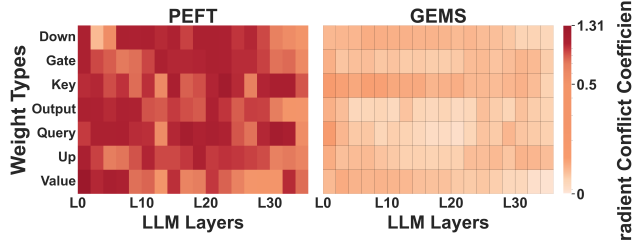


Figure 4: Gradient conflict heatmap analysis of PEFT and GEMS using Qwen-3B on the Qilin dataset.

5.3 Analysis

After addressing RQ1, we conduct a detailed analysis of GEMS. Specifically, we examine the contributions of multi-subspace decomposition and null-space projection to its performance (see Section 5.3.1), evaluate its ability to mitigate gradient conflicts (see Section 5.3.2) and preserve user intent understanding (see Section 5.3.3), and analyze its sensitivity to hyperparameters (see Section A.4).

5.3.1 Ablation study (RQ2). To better understand the contribution of each component within GEMS, we conduct an ablation study by progressively removing its two core modules: multi-subspace decomposition and null-space projection. Figure 3 presents the ablation experimental results for both backbone models also compared with strong unifying S&R baseline Sem-BSR, revealing the following key findings: (1) **Effect of multi-subspace decomposition:** When we disable the multi-subspace decomposition and instead optimize over a single shared subspace, we observe a substantial degradation in performance across both S&R, which confirms that explicitly disentangling shared and task-specific signals into complementary subspaces is essential for mitigating interference and maintaining stable optimization. (2) **Effect of null-space projection:** We then remove the null-space projection step, allowing updates to freely drift within the full parameter space. In this setting, the model achieves moderate improvements over baselines but still lags behind the full GEMS, which highlight the importance of constraining updates to remain orthogonal to pre-trained knowledge representations in order to preserve the LLM’s language understanding ability. (3) **Effect of subspace tuning.** We also evaluate the version that applies only subspace tuning, removing both modules. Overall, subspace tuning demonstrates strong performance by optimizing within an effective low-rank subspace. However, in certain scenarios, gradient conflicts diminish this advantage, leading to cases where Sem-BSR outperforms it, further underscoring the effectiveness of Multi-Subspace Decomposition.

5.3.2 Gradient conflict analysis (RQ3). In this section, we empirically analyze gradient conflicts in GEMS to assess how effectively our method alleviates them. We quantify the degree of conflict using the **Gradient Conflict Coefficient** (ρ), which measures how strongly the task gradients align or oppose each other during training. Given the gradients of the search task g_{src} and the recommendation task g_{rec} , ρ is defined as:

$$\rho = 1 - \frac{g_{\text{src}} \cdot g_{\text{rec}}}{\|g_{\text{src}}\| \|g_{\text{rec}}\|}. \quad (21)$$

Table 3: User intent understanding preservation analysis under Qwen-3B. We report the percentage of “correct-before → incorrect-after” (lower is better). Δ denotes the absolute reduction compared to the BSR baseline.

Dataset	Task	PEFT	Ours	Δ
Qilin	Rec.	21.1%	10.6%	-10.5%
	Search	24.8%	12.9%	-11.9%
Amazon	Rec.	18.9%	7.9%	-11.0%
	Search	26.2%	11.7%	-14.5%

A higher coefficient indicates stronger conflicts, while a lower coefficient reflects better compatibility between the two objectives. As illustrated in Figure 4 and Figure 1(a), we obtain two key observations. (1) GEMS consistently achieves lower gradient conflict coefficients across all LLM layers compared with the PEFT baseline (*i.e.*, LoRA), indicating that it effectively mitigates competing optimization signals between S&R and facilitates smoother training dynamics. This finding validates the effectiveness of the multi-subspace decomposition mechanism. Quantitatively, GEMS alleviates over 85% of average conflict magnitudes across all weight types, reaching up to 88% (2) In PEFT, high-conflict regions predominantly occur in the *Query* and *Key* layers, where components that control attention alignment and are particularly sensitive to multi-task interference. In contrast, GEMS maintains uniformly low conflict magnitudes across layers, demonstrating more stable optimization behavior.

5.3.3 User intent understanding preservation analysis (RQ3). A key concern raised in the introduction is that adapting LLMs with PEFT in unified S&R can distort user intent understanding by overfitting to finetuned data and undermining the inherent language understanding and reasoning abilities of LLMs. To investigate whether GEMS better preserves such capability, we conduct an analysis comparing prediction consistency before and after fine-tuning. Concretely, we report the proportion of cases in which the base LLMs was correct but became incorrect after tuning. As shown in Table 3, PEFT method (*i.e.*, LoRA) exhibits a substantial share of disrupted cases across datasets, indicating that parameter-efficient updates can overwrite pre-trained representations in undesirable ways. In contrast, our method consistently reduces this disruption. The percentage of “correct-before, incorrect-after” cases is markedly lower under our methods for both S&R, suggesting the capability to preserving the models’s original language understanding an reasoning capability. Importantly, this preservation effect is not a byproduct of underfitting. The fine-tuned models using our method achieve superior task-specific performance relative to baselines. This suggests that our framework strikes a more favorable balance between specialization and retention of general capability of LLMs, which is essential for unifying S&R.

6 Conclusion

We have proposed GEMS, a Gradient Multi-Subspace Tuning framework that unifies search and recommendation. Extending subspace tuning, GEMS reduces tuning cost by projecting gradients into low-rank subspaces for optimization and mapping them back to

the full parameter space. It consists of two key components: (i) Multi-Subspace Decomposition, which mitigates gradient conflicts through disentangled shared and task-specific subspaces, and (ii) Null-Space Projection, which preserves general-domain knowledge by constraining updates to be orthogonal to the backbone's knowledge space. Across benchmark S&R tasks, GEMS consistently outperforms state-of-the-art baselines and demonstrates reduced gradient conflicts and mitigated semantic drift.

Our findings point to promising directions for applications that jointly exploit recommendation and search signals, enabling unified optimization within a single framework. However, the current design retains general-domain knowledge holistically rather than selectively preserving components most relevant to S&R, and relies on fixed subspace ranks that limit adaptive capacity. Future work will focus on selectively preserving general-domain knowledge pertinent to S&R to further reduce adaptation costs and on developing adaptive subspace learning mechanisms that dynamically adjust ranks as tasks evolve.

References

[1] Qingyao Ai, Yongfeng Zhang, Keping Bi, Xu Chen, and W Bruce Croft. 2017. Learning a hierarchical embedding model for personalized product search. In *SIGIR*. ACM, 645–654.

[2] Hyung Won Chung, Le Hou, Shayne Longpre, Barret Zoph, Yi Tay, William Fedus, Yunxuan Li, Xuezhi Wang, Mostafa Dehghani, Siddhartha Brahma, et al. 2024. Scaling instruction-finetuned language models. *Journal of Machine Learning Research* 25, 70 (2024), 1–53.

[3] Chuntao Ding, Zhichao Lu, Shangguang Wang, Ran Cheng, and Vishnu Naresh Boddu. 2023. Mitigating task interference in multi-task learning via explicit task routing with non-learnable primitives. In *CVPR*. IEEE, 7756–7765.

[4] Shihai Dou, Enyu Zhou, Yan Liu, Songyang Gao, Jun Zhao, Wei Shen, Yuhao Zhou, Zhiheng Xi, Xiao Wang, Xiaoran Fan, et al. 2023. Loramoe: Revolutionizing mixture of experts for maintaining world knowledge in language model alignment. *arXiv preprint arXiv:2312.09979* 4, 7 (2023).

[5] Yunshu Du, Wojciech M Czarnecki, Siddhant M Jayakumar, Mehrdad Farajtabar, Razvan Pascanu, and Balaji Lakshminarayanan. 2018. Adapting auxiliary losses using gradient similarity. *arXiv preprint arXiv:1812.02224* (2018).

[6] Junfeng Fang, Houcheng Jiang, Kun Wang, Yunshan Ma, Jie Shi, Xiang Wang, Xiangnan He, and Tat-Seng Chua. 2025. AlphaEdit: Null-Space Constrained Knowledge Editing for Language Models. In *ICLR*. OpenReview.net.

[7] William Fedus, Barret Zoph, and Noam Shazeer. 2022. Switch transformers: Scaling to trillion parameter models with simple and efficient sparsity. *Journal of Machine Learning Research* 23, 120 (2022), 1–39.

[8] Wenfeng Feng, Chuzhan Hao, Yuewei Zhang, Yu Han, and Hao Wang. 2024. Mixture-of-LoRAs: An Efficient Multitask Tuning Method for Large Language Models. In *LREC/COLING*. ELRA and ICCL, 11371–11380.

[9] Xiangnan He, Lizi Liao, Hanwang Zhang, Liqiang Nie, Xia Hu, and Tat-Seng Chua. 2017. Neural collaborative filtering. In *WWW*. ACM, 173–182.

[10] Edward J. Hu, Yelong Shen, Phillip Wallis, Zeyuan Allen-Zhu, Yuanzhi Li, Shean Wang, Lu Wang, and Weizhu Chen. 2022. LoRA: Low-Rank Adaptation of Large Language Models. In *ICLR*. OpenReview.net.

[11] Qiang Huang, Feng Huang, DeHao Tao, BingKun Wang, and YongFeng Huang. 2024. UNIFIT: A Unified Framework For Instruction Tuning To Improve Instruction Following Ability For Large Language Models. In *Proceedings of the Annual Meeting of the Cognitive Science Society*, Vol. 46.

[12] Diederik P. Kingma and Jimmy Ba. 2015. Adam: A Method for Stochastic Optimization. In *ICLR*.

[13] Dmitry Lepikhin, HyoukJoong Lee, Yuanzhong Xu, Dehao Chen, Orhan Firat, Yanping Huang, Maxxin Krikun, Noam Shazeer, and Zhifeng Chen. 2020. Gshard: Scaling giant models with conditional computation and automatic sharding. *arXiv preprint arXiv:2006.16668* (2020).

[14] Yongqi Li, Nan Yang, Liang Wang, Furu Wei, and Wenjie Li. 2024. Learning to rank in generative retrieval. In *AAAI*. AAAI press, 8716–8723.

[15] Gustavo Penha, Edoardo D'Amico, Marco De Nadai, Enrico Palumbo, Alexandre Tamborrino, Ali Vardasbi, Max Lefarov, Shaw Lin, Timothy Heath, Francesco Fabbri, et al. 2025. Semantic IDs for Joint Generative Search and Recommendation. In *RecSys*. 1296–1301.

[16] Gustavo Penha, Ali Vardasbi, Enrico Palumbo, Marco De Nadai, and Hugues Bouchard. 2024. Bridging Search and Recommendation in Generative Retrieval: Does One Task Help the Other?. In *RecSys*. ACM, 340–349.

[17] Jonas Pfeiffer, Aishwarya Kamath, Andreas Rücklé, Kyunghyun Cho, and Iryna Gurevych. 2021. AdapterFusion: Non-Destructive Task Composition for Transfer Learning. In *EACL*. ACL, 487–503.

[18] Colin Raffel, Noam Shazeer, Adam Roberts, Katherine Lee, Sharan Narang, Michael Matena, Yanqi Zhou, Wei Li, and Peter J Liu. 2020. Exploring the limits of transfer learning with a unified text-to-text transformer. *Journal of machine learning research* 21, 140 (2020), 1–67.

[19] Shashank Rajput, Nikhil Mehta, Anima Singh, Raghunandan Hulikal Keshavan, Trung Vu, Lukasz Heldt, Lichan Hong, Yi Tay, Vinh Q. Tran, Jonah Samost, Maciej Kula, Ed H. Chi, and Mahesh Sathiamoorthy. 2023. Recommender Systems with Generative Retrieval. In *NeurIPS*.

[20] Victor Sanh, Albert Webson, Colin Raffel, Stephen H. Bach, Lintang Sutawika, Zaid Alyafei, Antoine Chaffin, Arnaud Stiegler, Arun Raja, Manan Dey, M Saiful Bari, Canwen Xu, Urmish Thakker, Shanya Sharma Sharma, Eliza Szczęcza, Taewoon Kim, Gunjan Chhablani, Nihal V. Nayak, Debajyoti Datta, Jonathan Chang, Mike Tian-Jian Jiang, Han Wang, Matteo Manica, Sheng Shen, Zheng Xin Yong, Harshit Pandey, Rachel Bawden, Thomas Wang, Trishala Neeraj, Jos Rozen, Abheesht Sharma, Andrea Santilli, Thibault Févry, Jason Alan Fries, Ryan Teehan, Teven Le Scao, Stella Biderman, Leo Gao, Thomas Wolf, and Alexander M. Rush. 2022. Multitask Prompted Training Enables Zero-Shot Task Generalization. In *ICLR*. OpenReview.net.

[21] Zhang Shengyu, Dong Linfeng, Li Xiaoya, Zhang Sen, Sun Xiaofei, Wang Shuhe, Li Jiwei, Runyi Hu, Zhang Tianwei, Fei Wu, et al. 2023. Instruction tuning for large language models: A survey. *arXiv preprint arXiv:2308.10792* (2023).

[22] Teng Shi, Zihua Si, Jun Xu, Xiao Zhang, Xiaoxue Zang, Kai Zheng, Dewei Leng, Yanan Niu, and Yang Song. 2024. UniSAR: Modeling User Transition Behaviors between Search and Recommendation. In *SIGIR*. ACM, 1029–1039.

[23] Teng Shi, Jun Xu, Xiao Zhang, Xiaoxue Zang, Kai Zheng, Yang Song, and Enyun Yu. 2025. Unified Generative Search and Recommendation. *arXiv preprint arXiv:2504.05730* (2025).

[24] Zihua Si, Zhongxiang Sun, Xiao Zhang, Jun Xu, Xiaoxue Zang, Yang Song, Kun Gai, and Ji-Rong Wen. 2023. When search meets recommendation: Learning disentangled search representation for recommendation. In *SIGIR*. ACM, 1313–1323.

[25] Weiwei Sun, Lingyong Yan, Zheng Chen, Shuaiqiang Wang, Haichao Zhu, Pengjie Ren, Zhumin Chen, Dawei Yin, Maarten de Rijke, and Zhaochun Ren. 2023. Learning to Tokenize for Generative Retrieval. In *NeurIPS*.

[26] Wenjie Wang, Honghui Bao, Xinyu Lin, Jizhi Zhang, Yongqi Li, Fuli Feng, See-Kiong Ng, and Tat-Seng Chua. 2024. Learnable Tokenizer for LLM-based Generative Recommendation. *arXiv:2405.07314* (2024).

[27] Yizhong Wang, Swaroop Mishra, Pegah Alipoormolabashi, Yeganeh Kordi, Amirreza Mirzaei, Atharva Naik, Arjun Ashok, Arut Selvan Dhanasekaran, Anjana Arunkumar, David Stap, Eshaan Pathak, Giannis Karamanolakis, Haizhi Gary Lai, Ishan Purohit, Ishani Mondal, Jacob Anderson, Kirby Kuznia, Krima Doshi, Kuntal Kumar Pal, Maitreya Patel, Mehrad Moradshahi, Mihir Parmar, Mirali Purohit, Neeraj Varshney, Pani Rohitha Kaza, Pulkit Verma, Ravsehaj Singh Puri, Rushang Karia, Savan Doshi, Shailaja Keyur Sampat, Siddhartha Mishra, Sujan Reddy A, Sumanta Patro, Tanay Dixit, and Xudong Shen. 2022. SuperNaturalInstructions: Generalization via Declarative Instructions on 1600+ NLP Tasks. In *EMNLP*. ACL, 5085–5109.

[28] Jason Wei, Maarten Bosma, Vincent Y. Zhao, Kelvin Guu, Adams Wei Yu, Brian Lester, Nan Du, Andrew M. Dai, and Quoc V. Le. 2022. Finetuned Language Models are Zero-Shot Learners. In *ICLR*. OpenReview.net.

[29] Jason Wei, Yi Tay, Rishi Bommasani, Colin Raffel, Barret Zoph, Sebastian Borgeaud, Dani Yogatama, Maarten Bosma, Denny Zhou, Donald Metzler, Ed H. Chi, Tatsunori Hashimoto, Oriol Vinyals, Percy Liang, Jeff Dean, and William Fedus. 2022. Emergent Abilities of Large Language Models. *Transactions on Machine Learning Research* 2022 (2022).

[30] Shiguang Wu, Wende Wei, Mengqi Zhang, Zhumin Chen, Jun Ma, Zhaochun Ren, Maarten de Rijke, and Pengjie Ren. 2024. Generative retrieval as multi-vector dense retrieval. In *SIGIR*. ACM, 1828–1838.

[31] Yucheng Xia, Yuhang Liu, Tianhao Li, Sihan He, Hong Chang, Yaqing Wang, Yongqing Zhang, and Wenqi Ge. 2024. Assessing parameter efficient methods for pre-trained language model in annotating scRNA-seq data. *Methods* 228 (2024), 12–21.

[32] Jiayi Xie, Shang Liu, Gao Cong, and Zhenzhong Chen. 2024. UnifiedSSR: A Unified Framework of Sequential Search and Recommendation. In *WWW*. ACM, 3410–3419.

[33] Lee Xiong, Chenyan Xiong, Ye Li, Kwok-Fung Tang, Jialin Liu, Paul Bennett, Junaid Ahmed, and Arnold Overwijk. 2020. Approximate nearest neighbor negative contrastive learning for dense text retrieval. *arXiv preprint arXiv:2007.00808* (2020).

[34] Yaming Yang, Dilxat Muhtar, Yelong Shen, Yufeng Zhan, Jianfeng Liu, Yujing Wang, Hao Sun, Weiwei Deng, Feng Sun, Qi Zhang, et al. 2025. Mtl-lora: Low-rank adaptation for multi-task learning. In *AAAI*. Vol. 39. 22010–22018.

[35] Jing Yao, Zhicheng Dou, Ruobing Xie, Yanxiong Lu, Zhiping Wang, and Ji-Rong Wen. 2021. USER: A unified information search and recommendation model based on integrated behavior sequence. In *CIKM*. ACM, 2373–2382.

[36] Hamed Zamani and W. Bruce Croft. 2018. Joint Modeling and Optimization of Search and Recommendation. In *DESIRE*. Vol. 2167. CEUR-WS.org, 36–41.

[37] Xiaoyu Zhang, Ruobing Xie, Yougang Lyu, Xin Xin, Pengjie Ren, Mingfei Liang, Bi Zhang, Zhanhui Kang, Maarten de Rijke, and Zhaochun Ren. 2024. Towards empathetic conversational recommender systems. In *RecSys*. ACM, 84–93.

[38] Yuting Zhang, Yiqing Wu, Ruidong Han, Ying Sun, Yongchun Zhu, Xiang Li, Wei Lin, Fuzhen Zhuang, Zhulin An, and Yongjun Xu. 2024. Unified Dual-Intent Translation for Joint Modeling of Search and Recommendation. In *KDD*. ACM, 6291–6300.

[39] Jujia Zhao, Wenjie Wang, Chen Xu, Xiuying Chen, Zhaochun Ren, and Suzan Verberne. 2025. Unifying Search and Recommendation: A Generative Paradigm Inspired by Information Theory. *arXiv preprint arXiv:2504.06714* (2025).

[40] Jujia Zhao, Yumeng Wang, Zhaochun Ren, and Suzan Verberne. 2025. Model Meets Knowledge: Analyzing Knowledge Types for Conversational Recommender Systems. In *Proceedings of the Nineteenth ACM Conference on Recommender Systems*. 802–811.

[41] Jiawei Zhao, Zhenyu Zhang, Beidi Chen, Zhangyang Wang, Anima Anandkumar, and Yuandong Tian. 2024. GaLore: Memory-Efficient LLM Training by Gradient Low-Rank Projection. In *ICML*. OpenReview.net.

[42] Kai Zhao, Yukun Zheng, Tao Zhuang, Xiang Li, and Xiaoyi Zeng. 2022. Joint learning of e-commerce search and recommendation with a unified graph neural network. In *WSDM*. 1461–1469.

[43] Yujia Zhou, Jing Yao, Ledell Wu, Zhicheng Dou, and Ji-Rong Wen. 2023. WebUltron: An ultimate retriever on webpages under the model-centric paradigm. *IEEE Transactions on Knowledge and Data Engineering* 36, 9 (2023), 4996–5006.

Table 4: Statistics of two datasets. #Inter-S and #Inter-R denote the interaction number of search behavior and recommendation behavior, respectively.

Dataset	#User	#Item	#Inter-S	#Inter-R	Density-S	Density-R
Qilin	3,816	275,515	16,626	101,085	0.00158%	0.00962%
Amazon	62,909	158,296	389,342	451,301	0.00391%	0.00453%

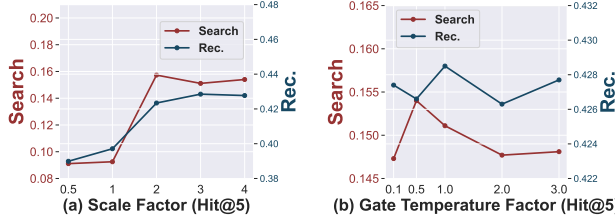


Figure 5: Hyperparameter analysis on Qilin.

Algorithm 1 Training algorithm of GEMS

Require: LLM Layer weight $W \in \mathbb{R}^{m \times n}$ ($m \leq n$). Step size η , scale factor α , rank r , SVD refresh step T_{svd} , gate temperature factor τ , pretrained basis $\mathbf{U}_{\text{ref}}^k$.

```

1: Initialize moments  $M^{(\text{src})}, M^{(\text{rec})}, M^{(\text{shared})} \in \mathbb{R}^r \leftarrow 0$ 
 $V^{(\text{src})}, V^{(\text{rec})}, V^{(\text{shared})} \in \mathbb{R}^r \leftarrow 0$ 
2:  $t \leftarrow 0$ 
3: function SUBSPACETUNE(type, g, t)
4:   ▷ Look up and maintain per-type states:  $U_r^{(\text{type})}, M^{(\text{type})},$ 
 $V^{(\text{type})}$ 
5:   if  $t \bmod T_{\text{svd}} = 0$  then refresh  $U_r^{(\text{type})}$  via SVD as in Eq.(2)
6:   Compute  $\Delta_t^{(\text{type})}$  according to Eq.(2)-(8) given g
7:   return  $\Delta_t^{(\text{type})}$ 
8: function NULLPROJECT( $\Delta, \mathbf{U}_k$ )
9:   return  $(\mathbf{U}_k \mathbf{U}_k^T) \Delta$  ▷ null-space projection
10: repeat
11:   Sample mini-batch  $\{(u, H_u, q, i^*)\}_{b=1}^B$  ▷  $q \neq \emptyset$ : search;
 $q = \emptyset$ : recommendation
12:   Compute  $\mathcal{L}_{\text{src}}, \mathcal{L}_{\text{rec}}$  with  $x = \text{format}(H_u, q)$ 
13:   Compute  $\mathbf{G}_t^{\text{src}}, \mathbf{G}_t^{\text{rec}}, \mathbf{G}_t^{\text{shared}}$  according to Eq.-(11)-(11)
14:    $\Delta_t^{\text{src}} \leftarrow \text{SUBSPACETUNE}(\text{src}, \mathbf{G}_t^{\text{src}}, t)$ 
15:    $\Delta_t^{\text{rec}} \leftarrow \text{SUBSPACETUNE}(\text{rec}, \mathbf{G}_t^{\text{rec}}, t)$ 
16:    $\Delta_t^{\text{shared}} \leftarrow \text{SUBSPACETUNE}(\text{shared}, \mathbf{G}_t^{\text{joint}}, t)$ 
17:    $\Delta_t^{\text{fuse}} \leftarrow \Delta_t^{\text{shared}} + \alpha_{\text{src}} \Delta_t^{\text{src}} + \alpha_{\text{rec}} \Delta_t^{\text{rec}}$  ▷ adaptive fusion
18:    $\Delta_t^{\text{final}} \leftarrow \text{NULLPROJECT}(\Delta_t^{\text{fuse}}, \mathbf{U}_{\text{ref}}^k)$  ▷ null-space projection
19:    $W \leftarrow W + \eta \Delta_t^{\text{final}}, t \leftarrow t + 1$  ▷ parameter update
20: until convergence
21: return  $W$ 

```

A Appendix

A.1 Training algorithm of GEMS

Algorithm 1 shows the training process of GEMS.

A.2 Data statistics

Table 4 shows the detailed statistics of the datasets used in our experiments.

A.3 Efficiency analysis

We analyze the memory and optimization efficiency of our method compared with the widely used PEFT method – LoRA [10]. Let a linear transformation layer in LLMs have a weight matrix $W \in \mathbb{R}^{m \times n}$ with $m \leq n$. The memory costs can be decomposed into two parts: (1) *weights*, which must be stored and accessed during both training and inference, and (2) *optimizer states*, which are maintained only during training.

For weights, GEMS does not introduce any additional low-rank factors beyond the original parameter matrix, resulting in a cost of mn . In contrast, LoRA introduces two low-rank matrices $A \in \mathbb{R}^{m \times r}$ and $B \in \mathbb{R}^{r \times n}$, requiring an additional $mr + nr$ parameters on top of W .

For optimizer states, our method maintains first- and second-order momentum estimates for three subspaces: one shared subspace of dimension r , and two task-specific subspaces of dimension $r/2$ each. This yields a total state size of

$$(mr/2 + nr) + (mr/2 + nr) + (mr + 2nr) = 2mr + 4nr.$$

By contrast, LoRA requires optimizer states for both A and B , leading to a total of $2mr + 2nr$.

Table 5 summarizes the comparison. Although our optimizer state is larger due to the multi-subspace design, our method achieves two clear advantages: (i) no additional weight parameters are introduced, which substantially reduces long-term memory costs and deployment overhead, and (ii) GEMS can naturally support both pre-training and fine-tuning, since it operates directly on the original parameter matrix W without introducing separate adaptation modules, whereas LoRA is limited to fine-tuning. Considering that weights dominate inference and deployment costs, our method provides overall higher efficiency in large-scale unified search and recommendation training.

Table 5: Efficiency comparison between our method and LoRA under $W \in \mathbb{R}^{m \times n}$, rank r .

	Ours	LoRA
Weights	mn	$mn + mr + nr$
Optimizer States	$2mr + 4nr$	$2mr + 2nr$
Multi-Subspace	✓	✗
Pre-Training	✓	✗
Fine-Tuning	✓	✓

A.4 Hyperparameter analysis (RQ4)

We analyze two critical hyperparameters: the scale factor α and the gate temperature factor τ . This analysis is performed on T5-base, presented in Figure 5. Our findings are as follows: (1) **Effect of α .** The scale factor α controls the strength of the low-rank update. When α is too small, insufficient task signals are injected, leading to under-updating and suboptimal performance on both S&R. Conversely, an excessively large α degrades performance, likely due to unstable training dynamics such as overshooting or diverging

from optimal basins. (2) **Effect of τ .** The temperature τ controls the sharpness of adaptive weighting. Very small τ yields near one-hot gating, suppressing one task, while very large τ degenerates to uniform weights. Intermediate τ achieves robust trade-offs, adaptively balancing S&R. (3) **Task-specific Optima.** We observe slight shifts

in the optimal hyperparameter ranges between S&R, reflecting their inherent task-specific characteristics. However, there exist broad overlapping regions where both tasks achieve strong performance, indicating that our framework is generally robust to hyperparameter settings.